ELSEVIER

Journal of Alloys and Compounds 413 (2006) 106–113

Journal of ALLOYS AND COMPOUNDS

www.elsevier.com/locate/jallcom

Directional metal-hydrogen bonding in interstitial hydrides II. Structural study of $HoNi_3D_x$ ($x = 0$, 1.3, 1.8)

Y.E. Filinchuk [a], D. Sheptyakov [b], K. Yvon [a,*]

[a] *Laboratoire de Cristallographie, Université de Genève, 24 quai E. Ansermet, CH-1211 Genève 4, Switzerland*
[b] *Laboratory for Neutron Scattering, ETHZ & PSI, CH-5232 Villigen PSI, Switzerland*

Received 9 June 2005; accepted 29 June 2005
Available online 15 August 2005

Abstract

The $HoNi_3$-hydrogen system has been re-investigated by neutron and synchrotron powder diffraction on deuterided samples. In contrast to previous reports at least four phases were identified, α–$HoNi_3D_x$ ($x \sim 0$), β$_1$-$HoNi_3D_{1.3}$, β$_2$-$HoNi_3D_{1.8}$ and γ-$HoNi_3D_x$, the latter being stable only at ∼100 bar D_2 pressure. Their structures were found to be non-centrosymmetric ($R3m$) rather than centrosymmetric ($R\bar{3}m$), and the Ni atoms to have pyramidal rather than planar trigonal deuterium atom coordinations. Thus, the $HoNi_3$-hydrogen system is very similar to the recently reported $ErNi_3$-hydrogen system (see part I, J. Alloys. Comp., in press) but unlike the cobalt-based RCo_3-hydrogen systems (R = Y, Er) in which the transition element tends to have octahedral hydrogen coordination. These results confirm that directional bonding effects between the transition element and hydrogen contribute in defining compositions and hydrogen atom distributions in "interstitial" metal hydrides.

Keywords: Hydrogen storage materials; Crystal structure and symmetry; Neutron diffraction

1. Introduction

In the first paper of this series the $ErNi_3$-hydrogen system was investigated by neutron powder diffraction (NPD) on deuterided samples [1]. At least three $ErNi_3D_x$ phases were found at deuterium compositions x∼1.3 (β$_1$), x∼2 (β$_2$) and x∼3.8 (γ), the latter phase being stable only under high deuterium pressure. Upon deuteration, the space group symmetry of the alloy (rhombohedral $PuNi_3$-type structure) decreased from centrosymmetric $R\bar{3}m$ to non-centrosymmetric $R3m$, and deuterium provided from two to four ligands of a Ni-centered NiD_4 tetrahedron. The tendency of nickel to adopt tetrahedral hydrogen configurations is known for nickel-based hydrides such as Mg_2NiH_4 and $LaMg_2NiH_7$ [2], but does not manifest itself in cobalt-based hydrides such as YCo_3H_x [3] in which cobalt tends to be octahedral surrounded by hydrogen. In view of these configurational differences around the transition element it was concluded [1] that the hydrogen atom distribution in the so-called "interstitial" metal hydrides cannot be rationalized by geometrical considerations alone, but needs to take into account directional bonding effects due to locally preferred metal-hydrogen configurations.

Clearly, this conclusion is at variance with results reported on the holmium containing nickel analogue $HoNi_3H_x$ that has been studied with respect to hydrogen pressure-composition-isotherms (PCT) [4], X-ray [5] and NPD [6]. The PCT data revealed an α-phase of composition $HoNi_3H_{0.6–0.7}$ at low hydrogen pressure and a β-phase of composition $HoNi_3H_{\sim 2}$ above 1 bar hydrogen pressure that was capable of dissolving up to an additional 0.5 hydrogen atom per formula unit (f.u.) under 30 bar hydrogen pressure [4]. A γ-phase of composition $HoNi_3H_{3.6}$ was obtained at 50 bar [5]. For the β-phase NPD data of relatively low resolution were refined on integrated intensities [6], based on a centrosymmetric model ($R\bar{3}m$) that displayed two partially occupied deuterium sites in nearly trigonal planar coordination around nickel.

* Corresponding author. Tel.: +41 22 379 6231; fax: +41 22 379 6864.
E-mail address: klaus.yvon@cryst.unige.ch (K. Yvon).

0925-8388/$ – see front matter © 2005 Elsevier B.V. All rights reserved.
doi:10.1016/j.jallcom.2005.06.068

Table 1
Atomic coordinates and thermal parameters for the deuterium-free $HoNi_3$ alloy (in bold, X-ray powder diffraction) and desorbed $HoNi_3D_x$ (in italic, synchrotron powder diffraction); space group $R\bar{3}m$

Atom	Wyckoff site	x	y	z	U_{iso} (Å^2)
Ho1	3*a*	0	0	0	**0.0115(5)**, *0.00298(12)*
Ho2	6*c*	0	0	**0.13902(5)**, *0.13947(2)*	**0.0136(4)**, *U(Ho1)*
Ni1	3*b*	0	0	1/2	**0.0018(11)**, *0.00247(19)*
Ni2	6*c*	0	0	**0.33290(11)**, *0.33247(8)*	**−0.0014(7)**, *U(Ni1)*
Ni3	18*h*	**0.4996(3)**, *0.49991(16)*	*−x*	**0.08199(6)**, *0.08217(4)*	**0.0021(5)**, *U(Ni1)*

Alloy sample. Main phase $HoNi_3$, $a = 4.95448(5)$, $c = 24.3262(3)$ Å, $c/a \sim 4.91$, $V = 517.132(10)$ Å^3, $R_B = 0.019$, $R_F = 0.020$, $\chi^2 = 2.48$, $R_p = 0.050$, $R_{wp} = 0.071$, 457 "independent" and 99 "effective" (accounting resolution [8]) reflections. Secondary phase Ho_2Ni_7 (18 wt.%): *R*-3*m*, $a = 4.9325(1)$, $c = 36.1646(6)$ Å, $V = 761.97(3)$ Å^3, $R_B = 0.091$.
Desorbed sample. Main phase $HoNi_3$, $a = 4.95740(2)$, $c = 24.34748(19)$ Å, $c/a \sim 4.91$, $V = 518.193(5)$ Å^3, $R_B = 0.034$, $R_F = 0.023$, $\chi^2 = 7.15$, $R_p = 0.045$, $R_{wp} = 0.060$, 295 "independent" and 144 "effective" reflections. Secondary phases: Ho_2Ni_7 (18 wt.%), *R*-3*m*, $a = 4.93527(8)$, $c = 36.1988(11)$ Å, $V = 763.56(3)$ Å^3, $R_B = 0.068$; Ho_2O_3 (∼1 wt.%).

These findings contrast sharply with those of the erbium analogue $ErNi_3D_x$, whose structure was found to be non-centrosymmetric (*R*3*m*) and displayed nearly fully occupied deuterium sites in a defect tetrahedral coordination around nickel [1].

The purpose of the present study was to re-investigate the $HoNi_3$-hydrogen system by high-resolution powder diffraction and full profile structure refinement methods. In view of the above-mentioned directional bonding effects due to locally preferred hydrogen configurations around nickel, the holmium and erbium based systems should in fact be quite similar. In the following it will be shown that this is indeed the case.

2. Experimental

2.1. Synthesis

Samples of nominal composition $HoNi_3$ were prepared by arc melting pieces of holmium (99.9%, JMC) and nickel (+99.9%, Alfa) under argon atmosphere. The ingots were annealed at 800 °C for 3 weeks in evacuated and argon filled quartz tubes and then quenched in cold water. No reaction was observed at the contact between the ingots and the walls of the quartz tube. Deuteration (D_2 gas, 99.8%, AGA) without preliminary activation was carried out in autoclaves at 100 °C and deuterium gas pressures of up to 30 bar for 3 days. Before opening the autoclaves they were slowly (∼24 h) cooled to room temperature. The reaction products were black powders that could be handled in air without detectable oxide formation. However, once exposed to air they desorbed and lost nearly all deuterium over a few days. Releasing the deuterium pressure resulted in a transformation within a few hours of the more deuterium-rich β_2- and γ-phases into the less deuterium-rich β_1- and α-phases (see Sections 2.3 and 2.5).

2.2. X-ray powder diffraction

The annealed $HoNi_3$ alloy was investigated by X-ray powder diffraction (Bruker D8 Advance diffractometer, $CuK_{\alpha 1}$ radiation, Bragg-Brentano geometry) in the 2θ range 10–120° ($d_{min} = 0.89$ Å) with a step size of 0.0144°. The sample contained a majority phase $HoNi_3$ (∼82%) that crystallized with the rhombohedral $PuNi_3$-type structure and a minority phase Ho_2Ni_7 (∼18%) having the rhombohedral Er_2Co_7-type structure [7]. Structure refinement was carried out with the FULLPROF SUITE program package [8] by accounting for severe texture along [0 0 1]. The background was described by a polynomial function and treated with a Fourier filtering technique. Refinement results are summarized in Table 1. Due to intense deuterium desorption and severe texture a detailed structural study of the deuterated samples $HoNi_3D_x$ on standard laboratory X-ray equipment was not feasible. However, these experiments revealed the existence of three different deuteride phases $HoNi_3D_x$ (referred to as β_1, β_2 and γ) having the cell parameters as summarized in Table 2. Compared to the deuterium-free alloy the cell volume has increased by ∼9–11% for the β_1- and β_2-phases, and by ∼24% for the γ-phase, while the *c/a* ratio has increased strongly for the β_1- and β_2-phases and weakly for the γ-phase. Phases with similar cell volumes and axial ratios, designated as β_1 and β_2, have been recently reported in the similar YCo_3D_x [3] and $ErNi_3D_x$ [1] systems. The β_1-phase of the present $HoNi_3D_x$ system was obtained in single-phase form at 15 bar deuterium pressure by cooling a sample slowly from 100 to 20 °C. Its cell parameters (Table 2) correspond to those of the previously reported "β-$HoNi_3D_{1.8}$" phase ($a \sim 4.99$, $c \sim 26.12$ Å, $c/a \sim 5.23$, $V = 563.3$ Å^3 [6]) whose deuteration conditions, however, were not specified. The β_2- and γ-deuterides were found to form at higher deuterium pressures but their equilibrium conditions were not examined. Interestingly, the minority phase with Er_2Co_7-type structure present in the alloy was no longer found in deuterided

Table 2
Cell parameters for deuterated $HoNi_3$ alloys as measured by X-ray powder diffraction

Phase	a (Å)	c (Å)	c/a	V (Å^3)
β_1-$HoNi_3D_x$	4.9858(4)	26.082(2)	5.23	561.49(7)
β_2-$HoNi_3D_x$	5.0265(3)	26.242(2)	5.22	574.20(6)
γ-$HoNi_3D_x$	5.258(1)	26.705(6)	5.08	639.4(2)

samples. This is presumably due to the effect of hydrogen-induced amorphization as reported in the La_2Ni_7-hydrogen system [9].

2.3. Neutron powder diffraction

A sample obtained at 30 bar deuterium pressure was immediately filled into a vanadium container, tightly sealed with indium wire and mounted on the HRPT diffractometer at SINQ (PSI; Villigen). A NPD pattern (called first pattern thereon) was collected under the following conditions: $\lambda = 1.15459(2)$ Å, 2θ range 6–164° ($d_{min} = 0.58$ Å), step size 0.1°, data collection time 6 h. It revealed the presence of ∼95% of β_2-phase and ∼5% of γ-phase. Then, deuterium was released from the sample in small portions by opening the vanadium container for about one minute and sealing it again. After letting the sample attain equilibrium for ∼8 h a short (∼10 min) NPD pattern was recorded to monitor the decomposition of the β_2-phase. After six desorption steps performed over four consecutive days an essentially single β_1-phase sample was obtained, and another NPD pattern (called second pattern thereon) was collected under the same conditions as before (data collection time ∼10 h). This pattern was essentially identical to that reported in [6] except that it had a much higher resolution and wider Q-range (0.63–10.8 $Å^{-1}$ as compared to 0.86–6.0 $Å^{-1}$ in [6]). The wavelength, zero-shift and instrumental resolution function (UVW in the Thompson-Cox-Hastings peak shape model) were calibrated by a silicon standard and fixed during structure refinement.

2.4. Structure refinement

The structures of the β_1- and β_2-deuterides were refined from the NPD patterns as follows. As a starting model the atomic parameters of γ-$ErNi_3D_{3.75}$ [1] as described in the centrosymmetric space group $R\bar{3}m$ were used with cell parameters derived from a profile fitting of the respective NPD patterns. For the β_1-deuteride (second pattern) only two out of six deuterium positions showed non-zero occupancies (D1, D2) and thus were retained in subsequent structure refinements. While the fit was relatively good ($R_B = 0.0497$, $R_F = 0.0282$, $\chi^2 = 14.2$, 33 parameters) the close proximity of the two nearly half-occupied sites (D1–D2 ∼ 1.55 Å, D1–D1 ∼ 1.97 Å) suggested a loss of inversion symmetry similar to that previously observed in the erbium system [1]. Consequently, the metal atom positions Ho2, Ni2 and Ni3 in space group $R\bar{3}m$ were split into pairs Ho21 + Ho22, Ni21 + Ni22 and Ni31 + Ni32, respectively, in space group $R3m$, and the two deuterium sites were split into four half-occupied deuterium sites that were pair-wise linked by inversion pseudo-symmetry. A preliminary unrestrained refinement of this non-centrosymmetric model converged at nearly full occupancy of two deuterium sites (D1: 0.93(2), D2: 0.90(5)) and zero occupancy for their inversion counterparts (0.03(2) and 0.04(4), respectively), thus confirming the nearly ordered deuterium atom arrangement of composition β_1-$HoNi_3D_{1.3}$. The cell parameters were consistent with those reported for $HoNi_3D_{1.8}$ [6] but much more precise. As shown in Table 3, the refinement of the non-centrosymmetic model (three Ho, five Ni, two almost fully occupied D sites) lead to a significantly better fit and smaller standard uncertainties for some positional parameters than the refinement of the centrosymmetric model (two Ho, three Ni, two partially occupied D sites). As to the closest D–D distances in the non-centrosymmetric model (D1–D1 ∼ 2.47 Å, D1–D2 > 3 Å) they are consistent with those in other ordered metal deuteride structures. The following 38 parameters were refined: 1 scale factor, 2 cell parameters, 2 profile parameters accounting isotropic Gaussian and Lorentzian sample broadening, 2 parameters for peak asymmetry at $2\theta < 30°$, 12 positional parameters, 6 isotropic thermal parameters and 2 occupancy factors for the D sites. One parameter, refined to 1.050(4), was introduced to correct for a minor preferred orientation along [001]. The background was described by a Fourier filtered polynomial with 10 refined parameters.

Table 3
Deuterium occupancies in β_1- and β_2-$HoNi_3D_x$, as refined in the average centrosymmetric $R\bar{3}m$ model and in the ordered non-centrosymmetric $R3m$ model

	β_1-$HoNi_3D_x$		β_2-$HoNi_3D_x$	
	$R\bar{3}m$	$R3m$	$R\bar{3}m$	$R3m$
D1	0.481(10)	0.954(17)	0.519(14)	1.02(3)
D2	0.372(15)	0.95(3)	0.419(18)	1.08(4)
D3			0.135(7)	0.227(15)
D4			0.111(9)	0.248(19)
χ^2	14.2	11.7	7.86	7.09
R_B	4.97	3.89	5.29	4.85

The same refinement strategy was used for the β_2-phase (the first NPD pattern) which was obtained in almost single-phase form (∼5% of γ-$HoNi_3D_x$) despite its relatively high equilibrium hydrogen pressure (∼30 bar). In contrast to the erbium analogue [1] which had to be refined in the centrosymmetric space group $R\bar{3}m$ due the lower quality of the NPD data (higher contribution of γ-$ErNi_3D_{3.8}$, ∼50%), the present β_2-phase could be successfully refined in $R3m$, see Table 3 for a comparison between the $R\bar{3}m$ and $R3m$ models. A total of four deuterium atom sites were identified and refined (D1 and D2 with full, and D3 and D4 with partial occupancies), yielding the composition β_2-$HoNi_3D_{1.8}$. The 46 refined parameters included those of the β_1-phase plus 2 occupational and 4 positional parameters for D3 and D4, one scale factor and two cell parameters for a small amount of secondary phase (γ-$HoNi_3D_x$). Final refinement results for the β_1- and β_2-phases are summarized in Table 4, and major Ni–Ni and Ni–D distances as compared to those in the alloy are listed in Table 5. The observed, calculated and difference NPD patterns are represented in Fig. 1. Similar to the X-ray patterns, a secondary phase with Er_2Co_7-type metal structure was not observed in the NPD patterns and therefore not included into the final refinements. Including such a phase with a fixed scale factor corresponding to an abundance of ∼10 wt.% impaired the refinement quality (higher χ^2 and

Table 4
Atomic coordinates and thermal parameters for β_1-$HoNi_3D_{1.3}$ (in bold) and β_2-$HoNi_3D_{1.8}$ (in italic) from NPD, space group *R*3*m*

Atom	Wyckoff site	*x*	*y*	*z*	U_{iso} (Å^2)	Occupancy
Ho1	3*a*	0	0	**−0.0026(7)**, *−0.0032(9)*	**0.0086(7)**, ***0.0133(11)***	
Ho21	3*a*	0	0	**0.1340(5)**, *0.1327(6)*	**0.0065(6)**, *0.0075(8)*	
Ho22	3*a*	0	0	**0.8726(5)**, *0.8737(6)*	*U*(Ho21)	
Ni1	3*a*	0	0	0.5000[a]	**0.0108(8)**, *0.0131(11)*	
Ni21	3*a*	0	0	**0.3298(5)**, *0.3283(6)*	**0.0130(5)**, *0.0174(9)*	
Ni22	3*a*	0	0	**0.6642(5)**, *0.6637(6)*	*U*(Ni21)	
Ni31	9*b*	**0.4998(10)**, *0.4991(11)*	*−x*	**0.0744(4)**, *0.0738(5)*	**0.0075(3)**, *0.0090(4)*	
Ni32	9*b*	**0.5021(11)**, *0.5034(11)*	*−x*	**0.9207(5)**, *0.9200(6)*	*U*(Ni31)	
D1	9*b*	**0.5018(12)**, *0.5007(14)*	*−x*	**0.1387(6)**, *0.1377(7)*	**0.0286(13)**, *0.0313(17)*	**0.954(17)**, *1.02(3)*
D2	3*a*	0	0	**0.2134(6)**, *0.2127(7)*	*U*(D1)	**0.95(3)**, *1.08(4)*
D3	9*b*	*0.5000*[a]	*0.5000*[a]	*−0.0163(14)*	*U*(D1)	*0.227(15)*
D4	9*b*	*0.855(4)*	*−x*	*0.0726(13)*	*U*(D1)	*0.248(19)*

β_1-$HoNi_3D_{1.3}$ (second NPD pattern): $a = 4.98868(6)$, $c = 26.0973(8)$ Å, $c/a \sim 5.23$, $V = 562.466(19)$ Å^3, $R_B = 0.0389$, $R_F = 0.0228$, $\chi^2 = 11.7$, $R_p = 0.0180$, $R_{wp} = 0.0238$, 427 "independent" reflections, 162 "effective" (accounting resolution [8]) reflections.
β_2-$HoNi_3D_{1.8}$ (first NPD pattern): $a = 5.03513(8)$, $c = 26.2971(11)$ Å, $c/a \sim 5.22$, $V = 577.38(3)$ Å^3, $R_B = 0.0485$, $R_F = 0.0276$, $\chi^2 = 7.09$, $R_p = 0.0181$, $R_{wp} = 0.0237$, 454 "independent" reflections, 160 "effective" reflections. Secondary phase γ-$HoNi_3D_x$ (4.6 wt.%): $a = 5.2698(13)$, $c = 26.662(19)$ Å, $c/a \sim 5.06$, $V = 641.2(5)$ Å^3, $R_B = 0.101$. All positions are fully occupied, except the deuterium sites.
[a] Fixed.

standard uncertainties) but did not invalidate the space group *R*3*m* and deuterium atom positions.

2.5. Structure characterization during desorption

Two samples were studied by synchrotron X-ray diffraction, one corresponding to the deuteride sample previously investigated by NPD, and the other to a freshly deuterated sample. The sample was kept after NPD in the sealed vanadium cylinder for one month and then studied on the Swiss-Norwegian beamline at ESRF (Grenoble, France) under the following conditions: $\lambda = 0.49886(3)$ Å, Debye–Scherrer geometry; 2θ range 3.5–44.3° ($d_{min} = 0.66$ Å), step size 0.006°. The cell parameters were close to those of deuterium-free $HoNi_3$, thus suggesting that the sample had lost most of its deuterium. Structure refinement results are included in Table 1, and diffraction patterns are shown on Fig. 2. Note that the sample contained ∼18% of a secondary phase with Er_2Co_7-type structure that has obviously recovered during deuterium desorption.

The second sample was prepared by charging the alloy under 100 bar deuterium pressure such as to favor the formation of the γ-$HoNi_3D_x$ phase. It was filled into an open quartz capillary and allowed to desorb deuterium near ambient conditions (36 °C) on the Materials Science beamline at SLS (PSI, Switzerland, $\lambda = 0.4335$ Å, Debye–Scherrer geometry). Some 300 high quality diffraction patterns were recorded in steps of 20 s by using a microstrip detector consisting of 15,000 Si-detector elements. Ten representative patterns, collected at time intervals from 1 to 20 min, are shown on Fig. 3. More detailed results on the $HoNi_3$-deuterium and the $ErNi_3$-deuterium systems will be reported elsewhere.

Table 5
Ni–Ni and Ni–D distances (Å) in the $HoNi_3$ alloy, β_1-$HoNi_3D_{1.27}$ and β_2-$HoNi_3D_{1.81}$ deuterides

$HoNi_3$ ($R\bar{3}m$)		β_1-$HoNi_3D_{1.27}$ (*R*3*m*)		β_2-$HoNi_3D_{1.81}$ (*R*3*m*)	
Ni1-Ni3	2.5060(15)	Ni1-Ni31	2.804(10)	Ni1-Ni31	2.838(12)
		Ni1-Ni32	2.688(11)	Ni1-Ni32	2.687(13)
		Ni1-3D1	1.628(8)	Ni1-3D1	1.647(10)
Ni2-Ni3	2.461(3)	Ni21-Ni31	2.492(14)	Ni21-Ni31	2.526(17)
Ni2-Ni3	2.448(3)	Ni21-Ni32	2.457(14)	Ni21-Ni32	2.468(17)
				Ni21-3D3	1.484(8)
		Ni22-Ni31	2.471(14)	Ni22-Ni31	2.491(18)
		Ni22-Ni32	2.458(15)	Ni22-Ni32	2.477(18)
				Ni22-3D3	1.496(9)
Ni3-Ni3	2.4719(17)	Ni31-Ni31	2.492(7)	Ni31-Ni31	2.531(8)
Ni3-Ni3	2.4825(17)	Ni31-Ni31	2.497(8)	Ni31-Ni31	2.504(8)
		Ni31-D1	1.678(18)	Ni31-D1	1.68(2)
				Ni31-2D4	1.56(2)
		Ni32-Ni32	2.463(7)	Ni32-Ni32	2.467(7)
		Ni32-Ni32	2.526(7)	Ni32-Ni32	2.568(7)
		Ni32-D2	1.804(13)	Ni32-D2	1.828(15)
				Ni32-D3	1.68(4)

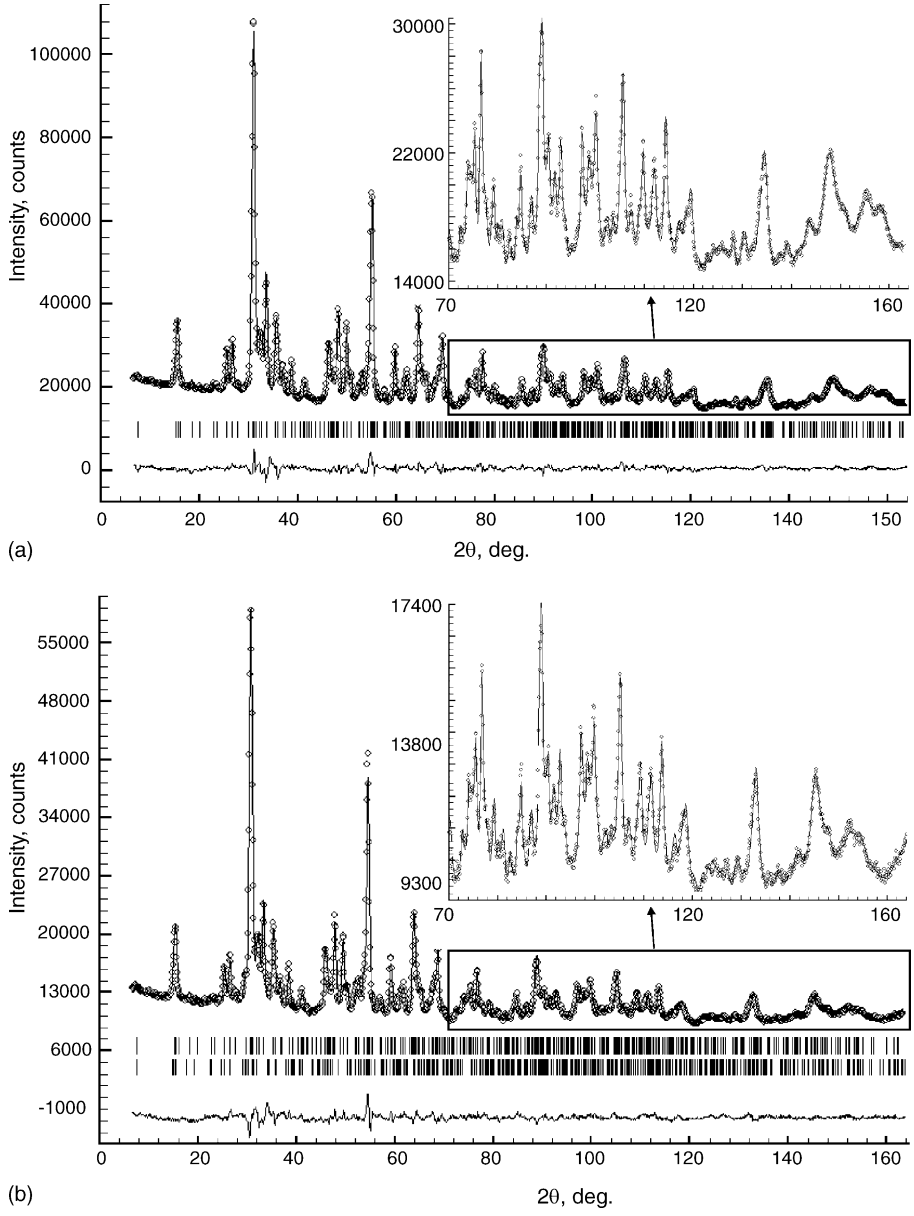

Fig. 1. Observed (points), calculated (line) and difference (bottom line) NPD patterns for β_1-$HoNi_3D_{1.3}$ (a) and β_2-$HoNi_3D_{1.8}$ (b); vertical bars indicate positions of Bragg peaks; second row of vertical bars in (b) indicates minority phase γ-$HoNi_3D_x$ (~5 wt.%).

3. Results and discussion

3.1. Phase relations

The $HoNi_3$-deuterium system contains at least four different phases, an α-phase at low deuterium content, two β-phases at intermediate deuterium content having the refined compositions β_1-$HoNi_3D_{1.27(2)}$ and β_2-$HoNi_3D_{1.81(3)}$, and a γ-phase of undetermined composition at high deuterium content. The α-phase contains only little deuterium as shown by the small difference in cell volume between the alloy $HoNi_3$ and the desorbed β_1-deuteride ($\Delta V = 1.06$ Å^3, see Table 1). It is not consistent with the previously reported relatively hydrogen-rich composition $HoNi_3H_{0.6–0.7}$ [4]. A comparison between the various cell parameters suggest that the β_1-phase identified in the present work corresponds to the previously reported β-phases "$HoNi_3H_{2.0}$" [4], "$HoNi_3H_{1.9}$" [5] and "$HoNi_3H_{1.8}$" [6], and the β_2-phase to the upper limit "$HoNi_3H_{2.8}$" attributed to the β-phase during PCT measurements under hydrogen pressure [4]. In other words, the hydrogen contents of the previously reported $HoNi_3H_x$ phases [6] and those marked on the PCT diagrams [4,5] are likely to be overestimated by 0.5–0.7 H/f.u. As to the γ-phase its existence is clearly seen on the in situ synchrotron powder diffraction patterns collected shortly after the high-pressure treatment (Fig. 3). Its hydrogen content as estimated from the increase in cell volume during hydrogenation suggests an approximate composition of γ-$HoNi_3H_{3.7}$, corresponding to

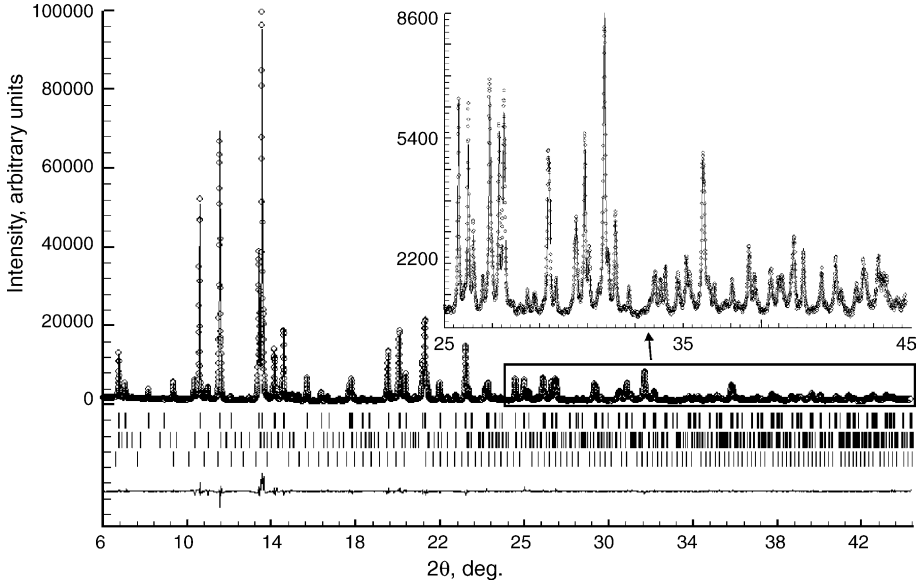

Fig. 2. Observed (points), calculated (line) and difference (bottom line) synchrotron powder diffraction patterns of a desorbed $HoNi_3D_x$ sample; rows of vertical bars indicate Bragg positions of majority phase $HoNi_3$ (top), minority phase Ho_2Ni_7 (middle) and impurity phase Ho_2O_3 (bottom).

a theoretical hydrogen storage efficiency of 1.07 wt.%. On desorption that phase transforms into the β_2-phase and then into a mixture of β_1- and β_2-phases that coexist. Since the cell parameters of these phases are similar, and the cell contraction upon the $\beta_2 \rightarrow \beta_1$ transition is nearly isotropic, the high resolution of the synchrotron experiment was essential to ascertain their existence as separate phases. Further desorption leads to the deuterium poor α-phase without formation of another intermediate deuteride.

3.2. Comparison between holmium and erbium systems

As expected, the $HoNi_3$-deuterium system is very similar to the analogous erbium system both with respect to the number and compositions of phases, cell parameters and cell ratios *c*/*a*. The values are compared in Table 6 and show that the parent rhombohedral cells of the alloys expand upon formation of the β_1-phases mainly along the *c* axis (in the hexagonal setting), then expand almost isotropically on the $\beta_1 \rightarrow \beta_2$ transitions, and finally expand mainly in the basal plane on transition to the γ-phases. As shown in a recent review [10] anisotropic expansion along the *c* axis in rhombohedral AB_3 hydrides with $PuNi_3$-type metal substructure can be attributed to hydrogen filling of interstitials in the AB_2 building blocks, and expansion in the basal plane to those in the AB_5 building blocks. Somewhat unexpectedly, the volume expansion per deuterium atom, ΔV/D-atom, is slightly bigger and the hydrogen equilibrium pressures slightly lower for the holmium containing deuterides compared to the erbium analogues.

3.3. Structure of β-phases

The structures of the β_1-$HoNi_3D_{1.3}$ and β_2-$HoNi_3D_{1.8}$ phases are isotypic with the erbium analogues β_1-$ErNi_3D_{1.3}$ and β_2-$ErNi_3D_{\sim 2}$, respectively [1]. In contrast to the deuterium free alloys they are non-centrosymmetric. The β_1-$HoNi_3D_{1.3}$ phase displays a largely ordered deuterium atom

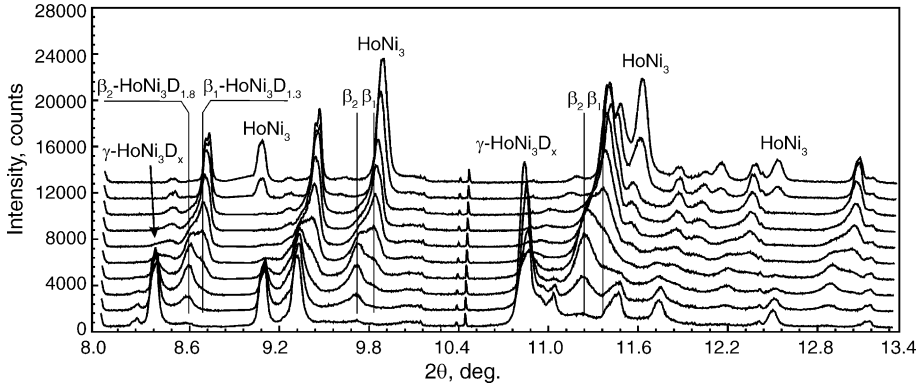

Fig. 3. In situ synchrotron powder diffraction patterns upon desorption of γ-$HoNi_3D_x$ deuteride ($\lambda = 0.4335$ Å, 36 °C); bottom pattern: γ-phase, top pattern: alloy.

Table 6
Cell expansion upon deuteration in the $HoNi_3$-D_2 and $ErNi_3$-D_2 [1] systems[a]

Phase	a (Å)	c (Å)	c/a	V (Å^3)	ΔV/D-atom (Å^3)
$HoNi_3$ alloy	4.95448(5)	24.3262(3)	4.91	517.132(10)	
$ErNi_3$ alloy	4.94794(7)	24.2909(5)	4.91	515.02(2)	
β_1-$HoNi_3D_{1.27(2)}$	4.98868(6)	26.0973(8)	5.23	562.466(19)	3.97(6)
β_1-$ErNi_3D_{1.23(1)}$	4.97180(7)	25.9012(5)	5.24	554.47(2)	3.56(3)
β_2-$HoNi_3D_{1.81(3)}$	5.03513(8)	26.2971(11)	5.22	577.38(3)	3.70(6)
β_2-$ErNi_3D_{1.97(4)}$	5.0456(3)	26.157(3)	5.18	576.70(8)	3.48(7)
γ-$HoNi_3D_x$	5.2698(13)	26.662(19)	5.06	641.2(5)	–
γ-$ErNi_3D_{3.75(8)}$	5.2398(3)	26.605(2)	5.08	632.60(8)	3.48(7)

[a] Values from NPD except for the $HoNi_3$ alloy (X-ray data).

distribution (for occupancy factors see Table 3) that contrasts with the disordered distribution reported for β-$HoNi_3D_{1.8}$ [6]. One deuterium site (D1) is at the centre of a trigonal-bipyramid of metal atoms (base: 1Ho + 2Ni; apices: 2Ho) and corresponds to the 18h_7 site recently identified by Liu et al. in the centrosymmetric cobalt analogue YCo_3D_x [2]. It differs from the previously suggested site in the centrosymmetric model of β-$HoNi_3D_{1.8}$ (18h_1 with occupancies of 64% [6]). The other site (D2) is at the centre of a metal tetrahedron (3 Ho + 1 Ni) and can be considered as an ordered derivative of the partially occupied 6c_1 site (78%) in the centrosymmetric model as suggested in [6]. Full occupancy of both sites corresponds to a limiting composition for the β_1-phase of $HoNi_3D_{1.33}$, as compared to the previously reported compositions β-$HoNi_3D_{1.8–2.0}$ [3–6] which have been overestimated. Deuterium interacts only with two out of five independent nickel atoms (Table 4): Ni32 has one D2 ligand at 1.80 Å, and Ni1 three D1 ligands at 1.63 Å, the latter forming a trigonal pyramid with nearly tetrahedral angles of 101.5(6)°. As shown in Fig. 4 this configuration contrasts with the reported trigonal planar configuration [6].

The β_2-$HoNi_3D_{1.8}$ phase displays four deuterium sites of which two (D1, D2) correspond to those in the β_1-phase and are nearly fully occupied, and two (D3, D4) are additional sites that are partially occupied (23–25%) similar to those in the erbium analogue β_2-$ErNi_3D_{2.0}$ (27–30% [1]). While D3 is at the centre of a trigonal-bipyramid of metal atoms (base: 3 Ni; apices: 2 Ho) and corresponds to the 18h_8 position reported for the first time for the centrosymmetric model of the erbium analogue [1], D4 is at the centre of a metal tetrahedron (2Ho + 2Ni) and corresponds to a 18h_2 site reported earlier [6]. In contrast to the β_1-phase all nickel atoms interact with deuterium. As shown in Fig. 5 and Table 5,

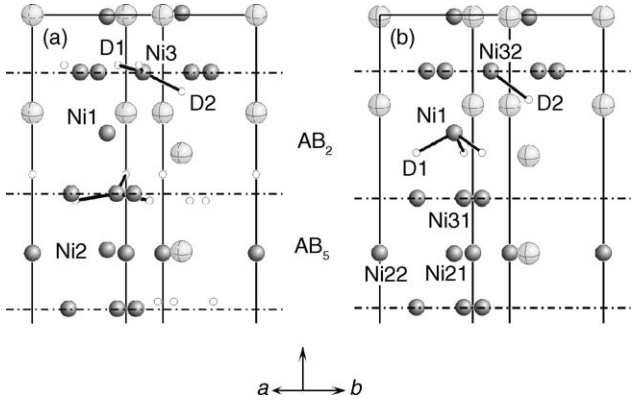

Fig. 4. Crystal structure fragment of β_1-$HoNi_3D_x$ (a) as determined in [6] for a centrosymmetric model of composition $HoNi_3D_{1.8}$ (*R*-3*m*, occupancies: D1: 64%, D2: 78%); and (b) for a non-centrosymmetric model of composition β_1-$HoNi_3D_{1.3}$ (*R*3*m*, D1 and D2 nearly fully occupied) as revised in this work; D-atom environments around Ni are highlighted.

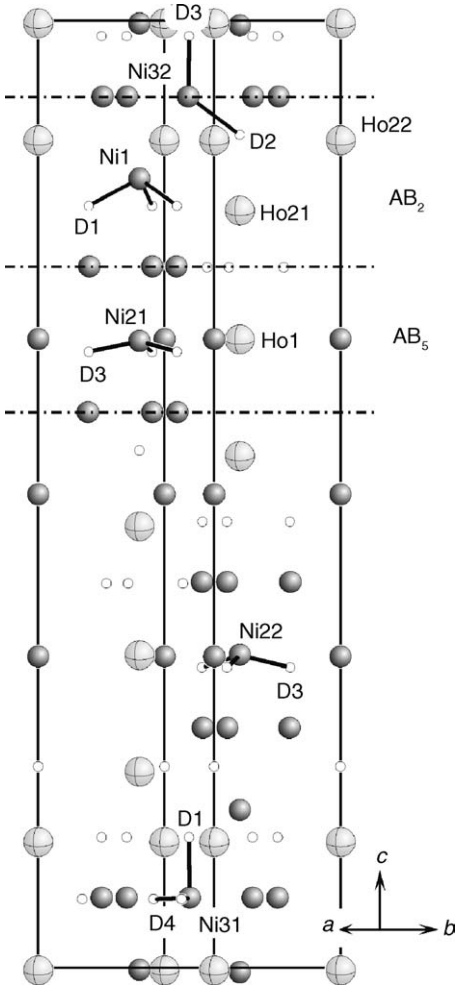

Fig. 5. Crystal structure of non-centrosymmetric β_2-$HoNi_3D_{1.8}$ (*R*3*m*, D1 and D2 nearly fully occupied, D3 and D4 partially occupied); D-atom environments around Ni are highlighted.

Ni1 has one D-site at 1.65 Å (D1), Ni32 has two D-sites at 1.82 Å (D2) and 1.68 Å (D3) forming an angle of 125(3)°, and Ni21, Ni22 and Ni31 each have three D-sites at 1.48 (3 D3) Å, 1.50 (3 D3) Å, and 1.68 (D1) and 1.56 (2D4) Å, respectively, each in trigonal pyramidal configuration. The non-centrosymmetrical arrangement of deuterium atoms induces detectable displacements of the nickel atoms. While all Ni1–Ni3 distances in the alloy structure are equal, the Ni1–Ni31 distances in the β_1- and β_2-deuterides are notably longer than the Ni1–Ni32 distances (Table 5). Both distances increase upon transition from the alloy $HoNi_3$ to the deuteride β_1-$HoNi_3D_{1.3}$ along with an anisotropic cell expansion along the *c* axis. Only a small increase of nearly all Ni–Ni distances was observed upon transition from the β_1- to the β_2-phase (Table 5).

3.4. Comparison between nickel and cobalt analogues

The similarity between the nickel based RNi_3-hydrogen systems (R = Ho, Er) contrasts with their difference to the cobalt based RCo_3-hydrogen analogues (R = Y [2], Er). The main difference concerns the deuterium environment of the transition metal atom in the AB_2 building block, since nickel tends to have trigonal pyramidal and cobalt-octahedral hydrogen coordinations. This difference cannot be explained by geometrical considerations alone as with "interstitial" metal hydrides [11], because the hydrogen contents and transition metal radii are too similar for both types of systems. It confirms that directional metal-hydrogen bonding effects are instrumental in defining composition and hydrogen atom distributions in these type metal hydrides. The structural revision of the $HoNi_3$–deuterium system as presented in this work underlines the usefulness of this approach and demonstrates its predictive power.

Acknowledgements

This work was supported by the Swiss National Science Foundation and the Swiss Federal Office of Energy, and has been partially performed at the Swiss Spallation Neutron Source SINQ, Paul Scherrer Institute, Villigen, Switzerland.

References

[1] Y. Filinchuk, K. Yvon, J. Alloys. Comp. 404-405 (2005) 89–94, see book of abstracts of the International Symposium on Metal-Hydrogen Systems, etc, Crakow (Poland), 5–10 September 2004, 2006, p. 136.
[2] G. Renaudin, L. Guénée, K. Yvon, J. Alloys Comp. 350 (2003) 145.
[3] J. Liu, P.A. Georgiev, D.K. Ross, M. Roberts, K.A. Andersen, M. Telling, D. Fort, Phys. Rev. B, submitted for publication.
[4] V.V. Burnasheva, B.P. Tarasov, Russ. J. Inorg. Chem. 27 (1982) 1077.
[5] V.V. Burnasheva, B.P. Tarasov, Russ. J. Inorg. Chem. 27 (1982) 1378.
[6] V.V. Burnasheva, V.A. Yartys', S.P. Solov'ev, N.V. Fadeeva, K.N. Semenenko, Sov. Phys. Crystallogr. 27 (1982) 409.
[7] W. Ostertag, J. Less-Common Metals 13 (1967) 385.
[8] J. Rodriguez-Carvajal, FULLPROF SUITE, LLB Saclay & LCSIM Rennes, France, 2003.
[9] U.-I. Chung, J.-Y. Lee, J. Non-Cryst. Solids 110 (1989) 203.
[10] M. Latroche, A. Percheron-Guégan, J. Alloys Comp. 356–357 (2003) 461.
[11] D.G. Westlake, J. Less-Common Met. 75 (1980) 177.